SRTTU
Journal of Computational and Applied Research in Mechanical Engineering
jcarme.sru.ac.ir
JCARME
ISSN: 2228-7922

Research paper

Effect of valve plate silencing grooves on flow and pressure fluctuation in fixed displacement radial piston pump

Lokesh Kumar*, and Nimai Pada Mandal

Department of Mechanical Engineering, National Institute of Technology Patna, Patna, Bihar, 800005, India

Article info:

Article history:

Received: 00/00/0000
Accepted: 00/00/0018
Revised: 00/00/0000
Online: 00/00/0000

Keywords:

Radial piston pump,
Silencing grooves,
Valve plate,
Number of pistons,
Flow and pressure fluctuation.

***Corresponding author:**
lokesh.me15@nitp.ac.in

Abstract

This study focused on the flow and pressure fluctuations of a fixed displacement radial piston pump with a valve plate with silencing grooves, and the effect of the number of pistons (5, 6, and 7) has been investigated. Over the manifolds of the pump, valve plate silencing grooves are regarded as Top Dead Center (TDC) and Bottom Dead Center (BDC). The mathematical modelling is run in MATLAB Simulink. Analysing the flow characteristics and volumetric efficiency of the pump with and without silencing groove valve plate configuration of pump. The opening and closing area pattern of the kidney port is also analyzed.The percentage reduction of flow and pressure fluctuation with the silencing groove is 19% and 16.16%, respectively, for Z = 7, as compared to the model without silencing groove valve plate. The volumetric efficiency of the model with silencing groove valve plate is improved from 1% to 2% as compared to the model without silencing groove valve plate. The lower the flow and pressure fluctuation coefficients, higher the flow rate and volumetric efficiency of the pump for the model with silencing groove valve plate.

1. Introduction

The radial piston pump is widely used to deliver the pressurized oil in the hydraulic system. It has many advantages over another pump, such as higher displacement, higher operating pressure, and long life [1]. Thus, the role of the radial piston pump is significant in industrial applications; for example, widely used in machine tools, plastic and powder injection modelling system, and high-speed car drive system [2]. This pump operated at high pressure with less noise [2, 8], and its performance was highly dependent on non-dimensional parameters such as flow ripple and pressure fluctuations. Cai and Tian [3] worked on the shaft assignment of the radial piston pump and observed reduced noise, higher pressure, and improved service life. Li et al. [4] used a CFD and a mathematical model to analyses the piston chamber's oil pressure changes in the radial piston pump pre-compression area. They advised against making the bottom edge's length and span angle of the triangular groove too long or short. Guo et al. [5] studied the flow characteristics of a radial piston pump using the spool valve distribution technique and got reduced flow ripple. Zhao et al. [6] looked into the pentagon transmission mechanism of the pump piston, built a new double row radial piston pump, and studied flow fluctuation with greater volumetric efficiency. Tong et al. [7] studied the mechanism of the sliding valve distribution in the radial piston pump and analysed the pump's piston displacement and flow characteristics. Mandal et al. [9, 10] investigated the influence of silencing groove geometry on the valve plate on the piston kidney of the axial piston pump. Cho et al. [11] looked into dynamic modelling and developed valve plate indexing with appropriate parameters to manage the pressure in the piston's transition zone and study the pump's dynamic characteristics. Seeniraj et al. [12] investigated numerous valve plate design strategies for noise reduction. The estimated noise reduction without influencing volumetric efficiency by combing pre-compression grooves, pre-compression filter volume with groove, and decompression filter volume on the valve plate. To optimize the piston chamber capacity of the radial piston pump, eliminate noise, and pressure pulsation, Jiang et al. [13] conducted mathematical modelling in the pre-compression and decompression sectors. Huang et al. [14] studied pump supplied pressure pulsation and pump characteristics using variable displacement and speed pumps. Radial piston pumps are frequently employed as output motors for hydrostatic transmissions due to their higher efficiency and low starting torque. [15]

Furthermore, some experts have done studies on the hydraulic piston pump. Chao et al. [16] explained the mechanism of capped pistons and designed to improve the flow characteristics of axial piston pumps, enhance the volumetric efficiency, and reduce the flow and pressure ripple. Yin et al. [17] studied the pressure, flow, and vibration characteristics of a seawater axial piston pump. They estimated the pressure ripple and vibration of the pump under varied loading circumstances. Nizhegorodov et al. [18] built a radial-piston pump and used seismic testing to identify natural frequencies for flow control. Dong et al. [19] designed and manufactured the valve plate of the radial piston pump and improved the efficiency of the hydraulic transmission system. They also researched the control system on the variable-displacement radial piston pump and validated a good test result. Harrison and Edge [20] proposed that the reduction of airborne noise and pressure ripple has an effect on flow ripple. The flow ripple decreases as the pump frequency increases. Ye et al. [21] optimally designed the valve plate to effectively reduce noise from both fluid-borne noise and structure-borne noise sources. Additionally, they proposed that the ripples in the inlet and outlet flow as well as the pulsation of the swash plate moment have an impact on the noise of an axial piston pump. Zhou et al. [22] designed the valve plate for the even number of pistons in an axial piston pump and compared it to the odd number of pistons. They discovered a minor difference in pressure pulsation between the nine- and ten-piston model pumps, as well as a decrease in pressure pulsation with increasing operating pressure in general. Tao et al.[23] studied mathematical modelling and simulation to mechanically design a variable displacement radial piston pump to power a large-scale, multi-megawatt wind turbine. Zielinski et al.[24] developed a low-speed radial piston pump to examine the hydrostatic transmission system of a small hydropower facility. The flow parameters, performance, and efficiency of the pump have been determined using simulations and mathematical analysis. They indicated that the mechanism might operate more effectively at low speeds. Aligoodarz et al. [25] performed mathematical modelling and simulation of the centrifugal slurry pump to find the flow characteristics and efficiency of the slurry pump. The size, concentration, and density of the solid particles have an impact on the head and efficiency of this slurry pump.

In this study, the effect of the model of the valve plate with silencing grooves is analyzed on flow and pressure fluctuation, changing the number of pistons (5, 6, and 7) in the radial piston pump. Mathematical modeling is developed and simulated with MATLAB Simulink. Effect of valve plate with silencing grooves is observed better than the model of valve plate without silencing groove on opening /closing area of kidney port, flow rate, reduction in fluctuation coefficient, and volumetric efficiency.

2. Working principle of radial piston pump

A fixed displacement radial piston pump with structural details is shown in Fig. 1. The main components of the pump are cylindrical block (A), cylinder barrel (B), pump piston (C), compressed spring (D), stroking ring (E), delivery chamber (F), delivery port (G), kidney port (H), suction chamber (I), suction port (J), shaft (K) and silencing groove (M).

The cylinder block (A) is coupled with the driving shaft (K) and rotates in a journal bearing, while the pump piston (C) reciprocates with the compressed spring (D) in the cylinder barrel (B), which is positioned radially in the revolving cylinder block (A). The cylindrical geometry of valve plate and manifolds have higher and lower pressure chamber, which is referred to as delivery chamber (F) and suction chamber (I), and corresponding ports are delivery port (G) and suctions port (J). Reservoir and ports are connected through hosepipe externally. The stroking ring (E) is eccentrically fixed with the pump's outer casing and the cylindrical block. The center of eccentrically fixed stroking ring and cylinder block are 'Cs' and 'Cp,' respectively. The manifold chamber is internally connected with the kidney port (H) of the piston-cylinder barrel.

For the pump simulation, modelling considers an even and an odd number of pistons and the number of pistons is 5, 6, and 7 for different combinations with valve plates. Pistons are labelled with numbers 1 to 7, shown in Fig. 1, and pistons are reciprocating towards the center (Cp) of the rotating cylinder block (A) and inside the cylinder barrel (B) with deriving shaft (K). Pistons moves in the direction of Top Dead Centre (TDC) to Bottom Dead Centre (BDC), the volume of the cylinder barrel becomes reduced, and delivery stroke has been accomplished. Similarly, piston movement from BDC to TDC referred toward increment in volume and accomplished the suction stroke. At full load, the area of the needle valve is 16.67x10-6 m2.

3. Mathematical modeling

In Fig. 1, Structural details of the fixed displacement radial piston pump are shown. The center of the rotating cylinder block and the cylinder barrel are considered Cp. The stroking ring (E) is fixed with the pump's outer casing, and the center of the stroking ring is Cs. The distance between the center of the cylinder block and stroking ring is eccentricity along the y-direction, represented by the symbol e_s. The pistons reciprocate in the cylinder barrel, from zero to maximum from TDC to BDC, and the maximum reciprocating distance is twice the eccentricity. When the cylinder block rotates from point TDC to point, 'Os,' the angular position is covered for ith piston, with the constant rotating speed of the driving shaft. The pistons reciprocate inside the cylinder barrel with compressed spring and rotate closely with toughing stroke ring.

The i^{th} instantaneous pistons displacement of radial piston pump expressed by the Eq. (1) respectively as

$$S_{pi} = l_m - r_i \tag{1}$$

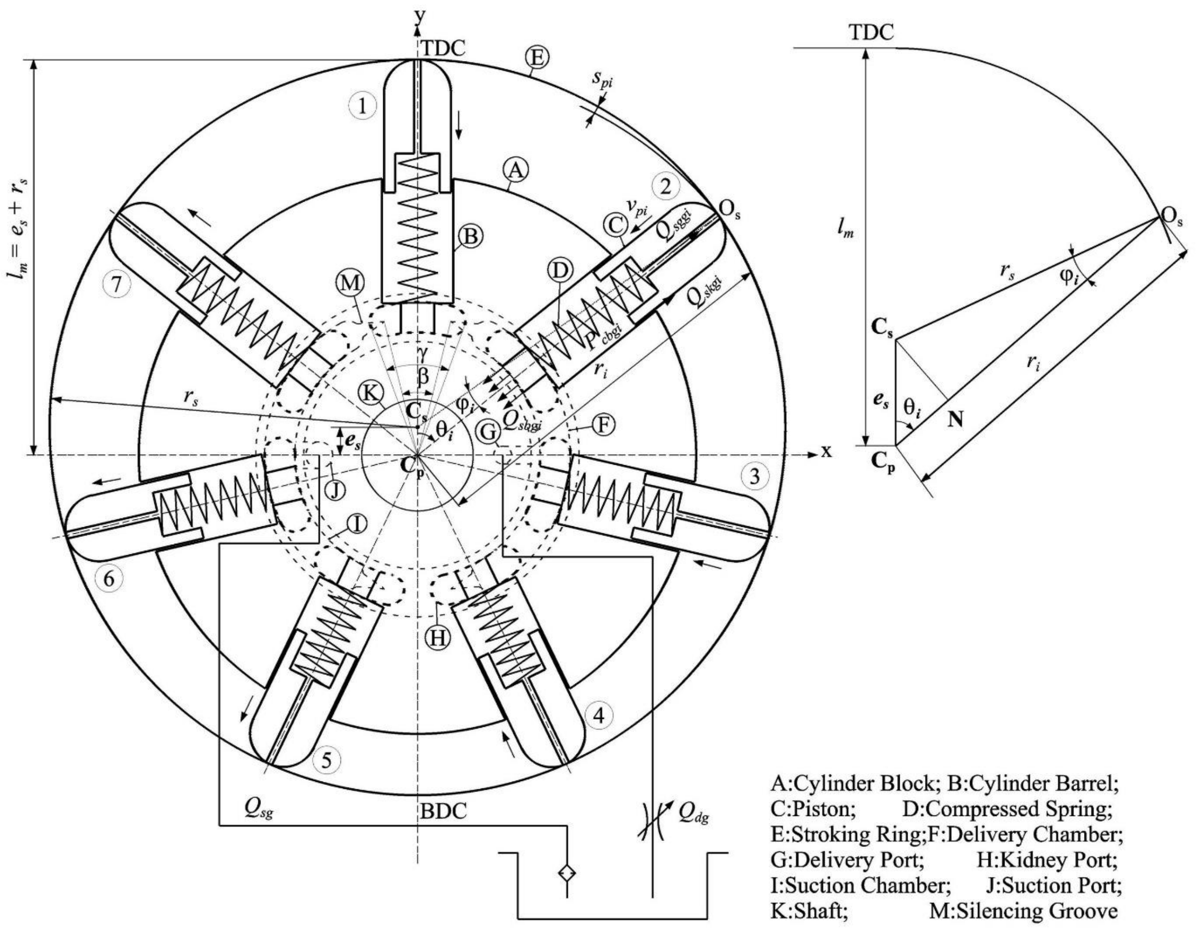

Fig. 1. Schematic diagram of radial piston pump with kinematic [2]

Where, the l_m is the length from centre of cylinder block C_p and the TDC of stroking ring r_i is the instantaneous linear position of piston at contact point O_s.

In Fig.1, Shown, the tringle $C_pC_sO_s$, the instantaneous linear position of the piston can be written as-

$$r_i = e_s\, cos\,\theta_i + r_s\, cos\,\varphi_i \tag{2}$$

Where, $\varphi_i = \sin^{-1}(\frac{e_s}{r_s}\sin\theta_i)$, $\theta_i = \theta + \varphi_i$,

$\varphi_i = 2\pi(i-1)/Z$,and Z is pistons number (5, 6 and 7)

The i^{th} instantaneous pistons velocity of pump expressed by the Eq. (3) [2] as

$$v_{pi} = e_s\omega(\sin\theta_i + \frac{e_s}{2r_s}\sin 2\theta_i) \tag{3}$$

Where, e_s is eccentricity between of stroke ring and cylinder block in m, r_s is radius of stroke ring in m, ω is shaft speed in rad/s and total number of pump piston is Z=5,6 and 7, offset angle in between the piston is φ=2π/Z.

Initially, all cylinder barrels are filled with liquid and the initial pressure is 0.2 MPa (same as reservoir pressure). The instantaneous pressure of the i^{th} cylinder barrel is the function of main flows, leakages, respective position and instantaneous volume of the piston. The rate of instantaneous pressure of i^{th} cylinder barrel for with silencing groove valve plate model can be written as in Eq. (4)-

$$\frac{dP_{cbgi}}{dt} = \kappa(Q_{sgi} + A_p v_{pi} - Q_{dgi} - Q_{skgi} - Q_{sggi} - Q_{sbgi})/(V_{pi} - A_p S_{pi}) \tag{4}$$

where P_{cbgi} is instantaneous cylinder barrel pressure, κ is bulk modulus, A_p is piston area, v_{pi} is instantaneous velocity of piston, Q_{sgi} is suction flow, Q_{dgi} is delivery flow, Q_{skgi}, Q_{sggi} *and* Q_{sbgi} are leakage flow and S_{pi} is instantaneous displacement for i^{th} piston. Similarly, instantaneous pressure rate of i^{th} piston for without silencing groove Eq. (5) is written as-

$$\frac{dP_{cbwi}}{dt} = \kappa(Q_{swi} + A_p v_{pi} - Q_{dwi} - Q_{skwi} - Q_{sgwi} - Q_{sbwi})/(V_{pi} - A_p S_{pi}) \quad (5)$$

where Q_{swi} is suction flows, and Q_{dwi} is delivery flow.

According to the elementary orifice flow Eq. described by Manring [15], the suction flows are Q_{sgi}, and Q_{swi} for with silencing groove and with silencing groove valve plate are as follows

$$Q_{sgi} = C_d A_{sgi} \sqrt{2(|P_{spg} - P_{cbgi}|)/\rho}\ sign(P_{spg} - P_{cbgi}) \quad (6)$$

$$Q_{swi} = C_d A_{swi} \sqrt{2(|P_{spw} - P_{cbwi}|)/\rho}\ sign(P_{spw} - P_{cbwi}) \quad (7)$$

Similarly, delivery flows are represented by Q_{dgi}, and $Q_{dwi,}$ for with silencing groove and without silencing groove valve plate model are as follows

$$Q_{dgi} = C_d A_{dgi} \sqrt{2(|P_{cbgi} - P_{sg}|)/\rho}\ sign(P_{cbgi} - P_{sg}) \quad (8)$$

$$Q_{dwi} = C_d A_{dwi} \sqrt{2(|P_{cbwi} - P_{sw}|)/\rho}\ sign(P_{cbwi} - P_{sw}) \quad (9)$$

where P_{spg}, and P_{spw} are suction manifold pressure, P_{sg}, and P_{sw} are delivery manifold pressure, A_{sgi}, and A_{swi} are instantaneous piston kidney area at suction side, A_{dgi}, and A_{dwi} are instantaneous piston kidney area at delivery side for with silencing groove and without silencing groove valve plate model respectively.

Instantaneous pressure rate of delivery manifold of pump for with silencing groove configuration can be written as

$$\frac{dP_{sg}}{dt} = (\sum_{i=1}^{5} Q_{dgi} - Q_{dg})\kappa / V_d \quad (10)$$

where Q_{dg} is the discharge through the needle and V_d is pipe line volume up to needle valve.

Similarly, supply pressure rate of delivery manifold chamber of pump for without silencing groove valve plate model using Eq. (10) replaced by symbol with P_{sw}, Q_{dwi} and Q_{dw}

The flow through the needle valve orifice for with silencing groove valve plate model can be written as in Eq. (11) [15]

$$Q_{dg} = C_d A_{ng} \sqrt{2(P_{sg} - P_r)/\rho}\ sign(P_{sg} - P_r) \quad (11)$$

Similarly, flow through the needle valve orifice Q_{dw} for without silencing groove valve plate model using Eq. (11) replaced by symbol with P_{sw} and A_{nw}. Where, A_{ng}, A_{nw} are the area of needle valve and P_r is reservoir pressure.

The Eqs. (4) and (5) shown for the valve plate with silencing groove and without silencing groove models are depended on leakage flows of pump, in between the annular gap of piston and barrel cylinder, central orifice of the piston and cylindrical valve plate and cylinder block. It can help the lubricating of systems and improve the anti-wear property. Equations from Eqs. (1-4) and Eqs. (12-16) is taken from Ivantysyn and Ivantysynova [2].

Leakage between the annular gap of i^{th} piston and barrel cylinder as- Ivantysyn and Ivantysynova [2].

$$Q_{skgi} = \frac{\pi d_k h_k^3}{12\mu l_k}(P_{cbi} - P_r) - \mu d_k h_k v_{pi}/2 \quad (12)$$

Leakage through the central orifice of i^{th} piston as- Ivantysyn and Ivantysynova [2].

$$Q_{sggi} = \frac{\pi d_d^4}{128\mu l_d}(P_{cbgi} - P_r) \quad (13)$$

Leakage between the annular gap of the cylindrical valve plate and i^{th} cylinder block as- Ivantysyn and Ivantysynova [2].

$$Q_{sbgi} = \frac{h_g^3}{12\mu}(P_i - P_r)\int d\delta / L \quad (14)$$

Where, d_k is diameter of cylinder, h_k is clearance between piston and barrel cylinder, P_{cbgi} is i^{th} cylinder barrel pressure, l_k is path length of piston in cylinder, μ is oil dynamic viscosity, l_d is length of central orifice of piston, d_d diameter of circular hole in piston, h_g is clearance between valve plate and cylinder block, L is width of manifold path is taken constant and the $d\delta$ is the function of angular position of width of manifold path.

4. Results and discussion

The instantaneous piston kidney area over the manifold is connected with the delivery side and the suction side area, shown in Fig. 2. The delivery side' piston kidney area is indicated with A_{dgi}, and A_{dwi} for with and without silencing groove, respectively, and its corresponding Expression follow in Eqs. (8) and (9).

Similarly, with and without silencing groove, piston kidney area in the suction side is represented with A_{sgi}, A_{swi}, and its in Eqs. (6) and (7), respectively.

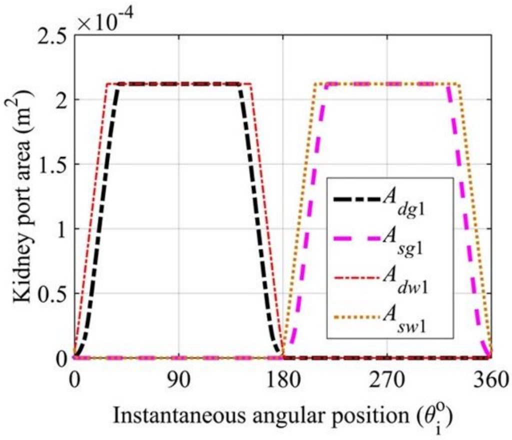

Fig. 2. Instantaneous kidney port area variation of 1st piston over the manifold.

The piston kidney area is calculated with parametric value of piston and kidney, which are mentioned in Table 1. Simulation is run in MATLAB and S- function is used for calculating the piston kidney area, for this calculation Runge-Kutta solver and $1e^{-7}$ s fixed time step is used. Half of the cycle works for the delivery port and another half for the suction port. This kind of cyclic opening and closing of the kidney port area continuously happens for every piston. In Fig. 2, up to 180-degree delivery port is opened, while this duration suction port is closed, after 180 degrees, suction port is opened, and delivery port gets closed. At 180 degrees, the main difference is that the silencing groove port area is open smoothly compared to without silencing groove, which has a sharp opening. Sharp opening promotes the fluctuations.

Initially, the piston is fitted with the compressed spring and reciprocating in the cylinder barrel and stroke ring. The cylinder block rotated with the pump shaft and piston reciprocating at a constant rotational speed in the cylinder barrel.The cylinder kidney and cylinder of the pump moved over the manifolds from the TDC (Top Dead Center), i.e., $\theta = 0^0$, to the BDC (Bottom Dead Center), i.e., $\theta = 180^0$, which is known as the Delivery manifold. The cylinder volume diminishes since the piston reciprocates within the cylinder barrel and fluid flow from the cylinder barrel to the delivery manifold. Taking after the completion of the half cycle, known as suction, from BDC (Bottom Dead Center), i.e., $\theta = 180^0$, to TDC (Top Dead Center), i.e., $\theta = 360^0$ or 0^0, since the volume of the barrel expanded with precise position in this area. Pump piston displacement affects the volumetric displacement of the pump. Instantaneous displacement and velocity (at 1500 rpm) curve of pump for a single cycle is shown in Fig. 3, and displacement and velocity of pump is calculated with the help of Eq. (1) and (3). The maximum displacement of the piston is twice the eccentricity in between the cylinder block and stroke ring.

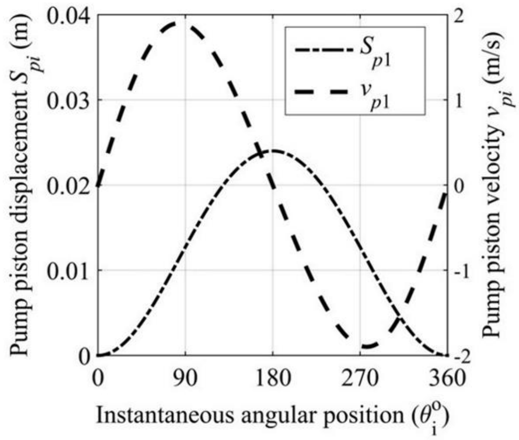

Fig. 3. Pump piston displacement and velocity curve at 1500 rpm.

The maximum pump piston velocity is 1.898 m/s. The pump cylinder barrel pressure is depended on the kinematic of the piston and fluid flow from manifolds to the cylinder barrel and vice versa as shown in Eq. (5). For the without silencing groove valve plate model of the pump shown in Fig. 4, the supply pressure

(P_{sw}), cylinder barrel pressure (P_{cbw1}), and suction pressure (P_{spw}) build-up in the delivery manifold, cylinder barrel, and suction- manifold, respectively. At needle valve orifice area 16.67×10^{-6} m^2.

These pressures are estimated at 1500 rpm with 7 pistons (Z=7) and 1.5 cycle for the valve plate without silencing groove. The maximum supply and cylinder barrel pressures are 10.2 MPa and 10.23 MPa, respectively.

Table 1. Parametric values used in simulation

Parameter	Value
Volumetric displacement (for Z=5, 6 and 7 pistons) [8]	63,76, and 89 cc/rev
Pitch radius of manifold (m)	0.05 m
Kidney port radius (m)	0.0043 m
Silencing groove angle (rad)	π/9
Kidney port angle (rad)	π/6
Angle of bridge gap (rad)	13π/90
Eccentricity in cylinder block (m)	0.012
Diameter of piston (m)	0.026
Initial volume of cylinder (m^3)	$1{,}5\times10^{-5}$
Control volume of delivery manifold (m^3)	3×10^{-4}
Control volume of suction manifold (m^3)	0.76
Dead volume of cylinder (m^3)	$2{,}5\times10^{-6}$
Reservoir pressure (MPa)	0.2
Coefficient of discharge of port -	0.61
Bulk modulus of fluid (N/m^2) [10]	$8{,}547\times10^{8}$
Density of fluid (kg /m^3) [10]	860
Needle valve dimeter on delivery side (m)	$4{,}6\times10^{-3}$

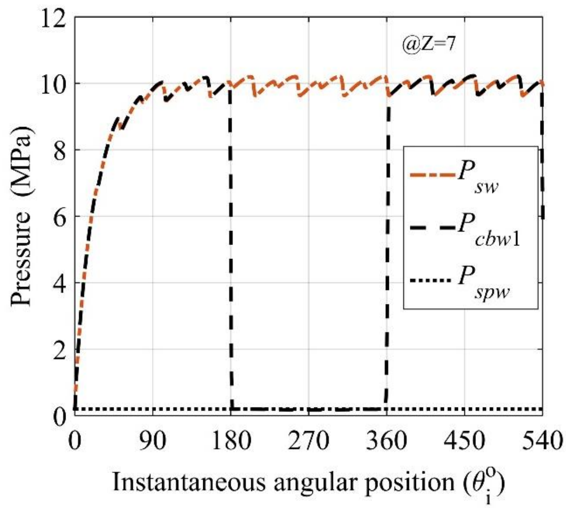

Fig. 4. Pressure characteristics of the pump, for without silencing groove model at 1500 rpm.

Eq. (11), for both the model with and without the silencing groove valve plate model at the same load area of the needle valve, defines the pump flow rate via the needle valve. Fig. 5, shows the instantaneous flow rate through a needle valve without a silencing groove at 1500 rpm, with varying number of pistons models (i.e, Z= 5,6, and 7) and a pressure of 10 MPa. With a silencing groove model, the mean flow rate is 93.23 lpm, 112.1 lpm, 130.7 lpm, while without a silencing groove; the mean flow rate is 92.6 lpm, 110.9 lpm, and 129.3 lpm, with 5, 6, and 7-piston model of the pump, respectively.

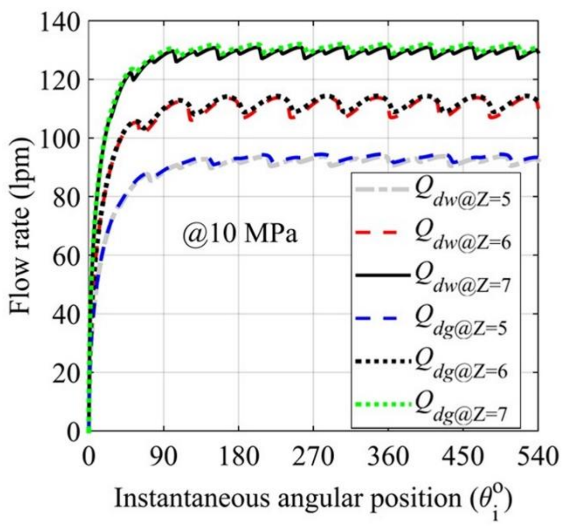

Fig. 5. Flow characteristics of the pump at 1500 rpm, for silencing groove model.

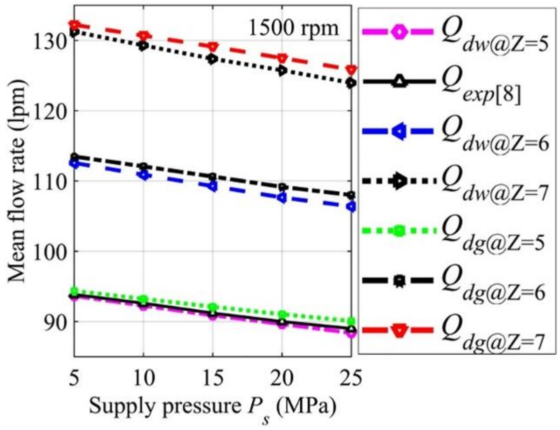

Fig. 6. Mean flow rate of the pump with supply pressure, at 1500 rpm.

This simulated radial piston pump result has been validated at a pressure ranging from 5 to 25 MPa, with a mean flow rate of the same volumetric displacement as the Moog pump [8] catalog, as illustrated in Fig. 6 at 1500 rpm. The simulated model's mean flow ranges from 88.39 lpm to 93.67 lpm for without silencing groove model at pressures ranging from 5 MPa to 25 MPa for 5 pistons, while the Moog pump's mean flow ranges from 93,85 lpm to 89 lpm [8].

For the 6-piston model without silence groove and silencing groove, mean flow ranges from 112.6 lpm to 106.4 lpm and from 113.5 lpm to 108 lpm, respectively. The mean flow rate is changed from 131.3 lpm to 124 lpm for the model without silencing groove and from 132.2 lpm to 125.9 lpm for the model with silencing groove, respectively, at the same pressure range depicted in Fig. 6.

The positive displacement piston pump creates internal vibration due to cyclic loads caused by the fluid pressure in the cylinder barrel, which is a liquid at high pressure. The pump manifolds transmit these vibrations to the remainder of the hydraulic system, creating vibration in the component and airborne noise from the pump valve plate geometry. The flow fluctuation of fluid through the valve plate geometry created two types of noise known as "airborne noise" and "structure-borne noise." The flow ripple in terms of non-dimensional parameter analysis at different speeds and the same load area of a needle valve for 5, 6, and 7 piston model at a rate of 1500 rpm, 1800 rpm, and 2100 rpm for without and with silencing groove, respectively, is shown in Fig. 7. For the silencing groove model, Ivantysyn and Ivantysynova [2] and Zhao et al. [6] define this ripple in the percentage of flow fluctuation coefficient, which is written as Eq. (15)-

$$\delta_{qg} = \{\{(Q_{dg})_{\max} - (Q_{dg})_{\min}\} / (Q_{dg})_{mean}\} \times 100\% \quad (15)$$

Where $(Q_{dg})_{\max}$ is maximum steady state flow rate, $(Q_{dg})_{\min}$ is minimum steady state flow rate, $(Q_{dg})_{mean}$ is mean steady state flow rate.

Similarly, the flow fluctuation coefficient (δ_{qw}) for without silencing groove using the Eq. (15) and calculate the flow coefficient at different speeds using different piston number models shown in Fig. 7. The theoretical flow rate fluctuation coefficient in terms of non-uniformity grade can be written as in Eq. (16)

$$\delta_{tq} = \varphi_Z \tan(\varphi_Z / 2) \quad (16)$$

Where $\varphi_Z = 180^o / Z$ in case of an even number of pistons, $\varphi_Z = 90^o / Z$ in case of an odd number of pistons, and φ_Z is the angle between minimum theoretical flow rate and maximum theoretical flow rate. The theoretical flow fluctuation coefficient values for 5, 6, and 7 piston models are 0.049, 0.14, and 0.025, respectively calculated by Ivantysyn and Ivantysynova [2]. As the number of pistons (odd or even) at the same speed increases, the theoretically and calculated simulated fluctuation coefficient decreases. The flow fluctuation coefficient for using an even number of pistons is mathematically larger than for using an odd number of pistons, as shown in Fig.7. The increased rotation speed of the pump has reduced flow fluctuation. The flow fluctuation coefficient is decreased for Z = 5, and the model of valve plate with a silencing groove compared to the without a silencing groove is 12.67%, 9.77%, and 8.4% at speeds of 1500 rpm, 1800 rpm, and 2100 rpm, respectively. Similarly, the flow fluctuation coefficient has been decreased for the silencing groove valve plate model as compared to the without silencing groove, which was 22%, 18.64%, and 16.76% for Z = 6, and 19%, 15.70%, and 13.94% for Z = 7 at the same speed.

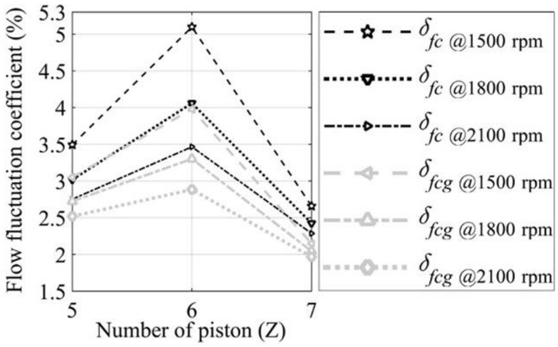

Fig. 7. Flow fluctuation coefficient with velocity variation.

The flow fluctuation coefficient at speed 1500 rpm with a different load pressure range from 5MPa to 25 MPa, considering the pump's 5, 6, and 7 piston model without silencing groove and with silencing groove model, respectively as shown in Fig. 8. The overall range of flow fluctuation is 9.5% to 2.06% for Z = 5, 6, and 7 at the pump's wide supply pressure range at 1500 rpm. The range of flow fluctuation within the silencing groove is from 4.03% to 2.33% for Z = 5, from 7.94% to 2.92% for Z = 6, and from 2.94% to 2.06% for Z = 7 at the same pressure range and speed. Similarly, for the model without a silencing groove, the range of flow fluctuation is 4.62%–2.75%, 9.5%–3.84%, and 3.71%–2.52% for Z = 5, 6, and 7, respectively.

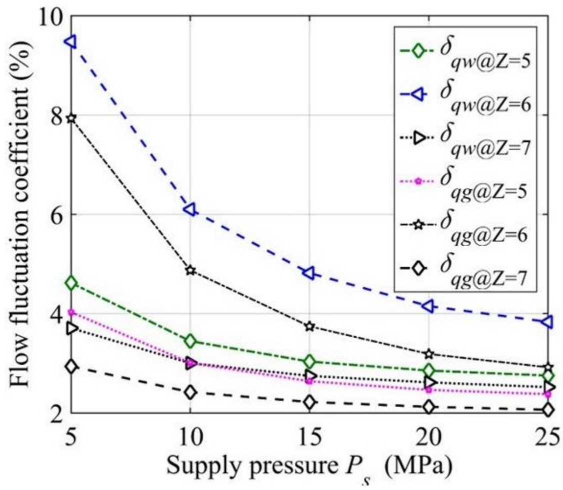

Fig. 8. Flow fluctuation coefficient of the pump at different load at a speed of 1500 rpm.

The fluid flow inside the pump component, such as fluid flow from the cylinder barrel to the manifolds and vice versa, combined with ripples to create the wave propagation. This propagation raises the system pressure on a regular basis, reducing pump life.The supply pressure fluctuation coefficient is a non-dimensional measure that expresses the pressure ripple. This analysis is performed at different speeds such as 1500 rpm, 1800 rpm, and 2100 rpm, for with and without silencing groove with the consideration of 5, 6, and 7 number of piston at fixed area of needle valve, shown in Fig 9.

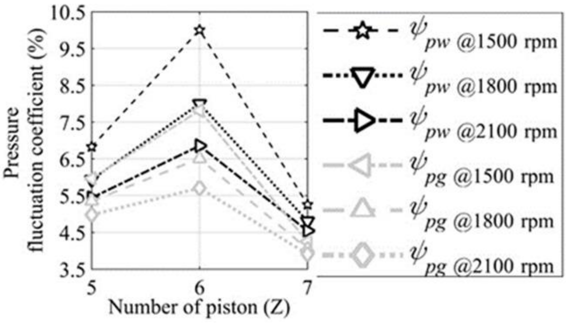

Fig. 9. Pressure fluctuation coefficient variation with number of pistons.

Huang et al [14] characterise the pressure ripple as a non-dimensional parameter that is represented by Eq. (17).

$$\psi_{pg} = \{\{(P_{sg})_{\max} - (P_{sg})_{\min}\} / (P_{sg})_{mean}\} \times 100\% \qquad (17)$$

Where, $(P_{sg})_{\max}$ is steady state maximum supply pressure of pump, $(P_{sg})_{\min}$ is steady state minimum supply pressure of pump, $(P_{sg})_{mean}$ is steady state mean supply pressure of pump. Similarly, the pressure fluctuation coefficient (ψ_{pw}) for without silencing groove model using by the Eq. (17) and calculate the pressure fluctuation coefficient at different speeds using different piston number models shown in Fig 9. The pressure fluctuation also decreased as the odd or even number of pistons increased. This fluctuation is reduced with increased pump speed. The reduction of the pressure fluctuation coefficient of the with silencing groove valve plate model compared to the without silencing groove model is 12.65%, 9.78%, and 8.49% using Z = 5, 6, and 7, respectively, at 1500 rpm. Similarly, the pressure fluctuation reduction in the model with silence groove versus the model without silence groove is 21.91%, 18.64%, and 16.8% for z = 6 and 16.16%, 15.73%, and 13.93% for z = 7 as shown in Fig 9.

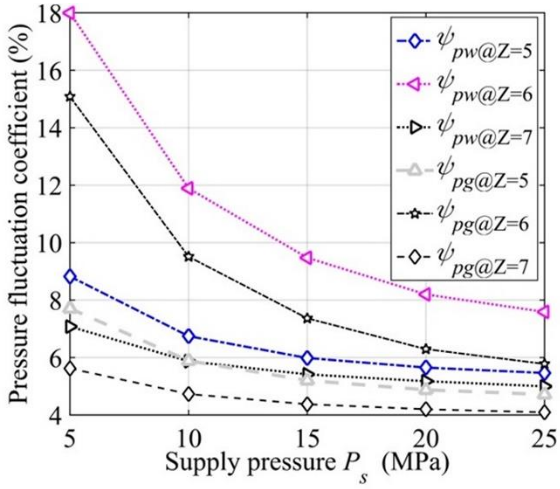

Fig. 10. Pressure fluctuation coefficient of the pump at different load at speed 1500 rpm.

The pressure fluctuation coefficient analysis at speed 1500 rpm, for further pressure, ranges from 5MPa to 25 MPa, considering the pump's 5, 6, and 7 piston model without silencing groove and silencing groove model, respectively, as shown in Fig. 10. This shows the pressure fluctuation coefficient is decreased with an increased range of supply pressure from the pump and a different number of pump pistons. The range of pressure fluctuation for the model with a silencing groove is 7.7% -4.72%, 15.08 -5.78%, and 5.623% -4.096% at the range of 5 MPa to 25 MPa pressure of the pump. Similarly, at the same wide range of pump pressure, the pressure fluctuation range for the pump model without a silencing groove is 8.83%-5.46%, 18%-7.58%, and 7.08%-5% for Z = 5, 6, and 7 pistons, respectively.

The pump capacity has been expressed in the term of volumetric efficiency and its Eq. is expressed in Eq. (18), for silencing groove model.

$$\eta_{vg} = (Q_{dg} / Q_t) \times 100\% \tag{18}$$

Similarly, the volumetric efficiency is represented as (η_{vw}), and discharge with $Q_{dw.}$ for without silencing groove model.

Theoretical flow rate of pump is expressed by the Eq. (19) [2].

$$Q_t = 0.5 Z \omega e_s \pi d_k^2 \tag{19}$$

Where, Q_{dg}, Q_{dw} are the mean flow rate of needle valve, with and without silencing groove model, respectively. Z is the number of pistons, ω is pump speed, e_s is the eccentricity between cylinder block and stroking ring and d_k is the diameter of piston of pump.

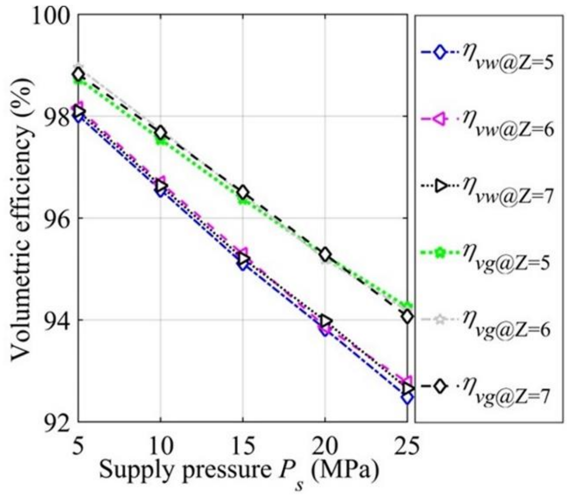

Fig. 11. Volumetric efficiency of the pump at different load at speed 1500 rpm.

Fig. 11 depicted the percentage of volumetric efficiency with different supply pressure at speeds of 1500 rpm considering with 5, 6, and 7 pistons of the model for with silencing groove and without silencing groove model respectively. The volumetric efficiency decreased with an increased supply pressure of the pump. The volumetric efficiency range between 98.95% to 92.49% at supply pressure ranged from 5 MPa to 25 MPa. Using a silencing groove improves volumetric efficiency over a valve plate model without a silencing groove for a wide range of supply pressure; the volumetric efficiency for the pump model with a silencing groove valve plate using Z = 5, 6, and 7 pistons is 98.74%-94.26%, 98.95%-94.18%, and 98.82%-94.07%, respectively. Similarly, for the same supply pressure range, the volumetric efficiency of the pump without a silencing groove valve plate using Z = 5, 6, and 7 pistons is 98.02%-92.49%, 98.16%-92.78%, and 98.1%-92.66%, respectively as shown in Fig. 11.

4. Conclusions

This study looks into the impact of valve plate silencing grooves on flow and pressure fluctuation in fixed displacement radial piston pumps with 5, 6, and 7 pistons, and the following conclusions are made-

- When silencing grooves are used, the opening and closing areas of the kidney port are smoother than in models without silencing groove valve plates.
- The effect was significantly less when comparing the flow rate with and without silencing grooves for an equivalent number of pistons.
- The mean flow rate is higher in every situation where silencing grooves are used, and a maximum flow rate of 7 pistons is obtained.
- At various speeds (1500, 1800, and 2100 rpm) and supply pressures, a minimum flow and pressure fluctuation are reported for seven pistons (up to 25 MPa). However, the highest fluctuation is found in the case of 6 piston numbers.
- When silencing grooves are used in the valve plate, volumetric efficiency is higher than in the model without silencing grooves, and maximum efficiency is found at 7 pistons in the silencing groove scenario.

References

[1] J. Yuehu, “New type of radial piston pump”, *National defence Ind. Press,* Beijing., pp. 6–8, (2012).

[2] J. Ivantysyn and M. Ivantysynova, *Hydrostatic Pumps and Motors Principles, Designs, Performance, Modelling, Analysis, Control and Testing;* 1st ed, Akad. Books Internat., New Delhi, pp.185-203, (2000).

[3] H. M. Cai and M. J. Tian, “Design of a shaft assignment radial piston pump”, *Adv. Mater. Res.*, Vol. 510, pp. 9-12, (2012).

[4] S. N. Li, L. J. Wei, X. P. Wei and J. H. Yang, “Change in Oil Pressure in Piston Chamber of a Radial Piston Pump Pre-Compression Area When Considering the Compressibility of Oil”, *Int. J. Fluid Mach. Syst.*, Vol. 13, No. 1, pp. 463-475, (2020).

[5] T. Guo, S. Zhao and C. Liu, “Study on flow characteristics and flow ripple reduction schemes of spool valves distributed radial piston pump”, *Proc. Inst. Mech. Eng., Part C: J. Mech. Eng. Sci.*, Vol. 231, No. 12, pp. 2291-2301, (2017).

[6] S. Zhao, T. Guo, Y. Yu, P. Dong, C. Liu and W. Chen, “Design and experimental studies of a novel double-row radial piston pump”, *Proc. Inst. Mech. Eng., Part C: J. Mech. Eng. Sci*, Vol. 231, No. 10, pp. 1884-1896, (2017).

[7] G. Tong, Z. Shengdun, Y. Yanghuiwen and S. Peng, “Design and theoretical analysis of a sliding valve distribution radial piston pump”, *J. Mech. Sci. Technol.*, Vol. 30, No. 1, pp. 327-335, (2016).

[8] Moog Radial Piston Pumps RKP Catalog, *Online referencing,* (2018).

[9] N. P. Mandal, R. Saha and D. Sanyal, “Theoretical simulation of ripples for different leading-side groove volumes on manifolds in fixed-displacement axial-piston pump”, *Proc. Inst. Mech. Eng., Part I: J. Syst. Control Eng.,* Vol. 222, No. 6, pp. 557-570, (2008).

[10] N. P. Mandal, R. Saha and D. Sanyal, “Effects of flow inertia modelling and valve-plate geometry on swash-plate axial-piston pump performance”, *Proc. Inst. Mech. Eng., Part I: J. Syst. Control Eng.*, Vol. 226, No. 4, pp. 451-465, (2011).

[11] J. Cho, X. Zhang, N. D. Manring and S. S. Nair, “Dynamic Modelling and Parametric Studies of An Indexing Valve Plate Pump”, *Int. J. Fluid Power,* Vol. 3, No. 3, pp. 37-48, (2002).

[12] G. K. Seeniraj, M. Zhao and M. Ivantysynova, “Effect of Combining Precompression Grooves, PCFV and DCFV on Pump Noise Generation”, *Int. J. Fluid Power,* Vol. 12, No. 3, pp. 53-63, (2011).

[13] W. Jiang, X. G. Qiu, G. Z. Chai and J. X. Zhou, "Research of the Pressure Pulsation within Piston Chamber in Radial Piston Pump", *Adv. Mater. Res.*, Vol. 69-70, pp. 626-630, (2009).

[14] J. Huang, Z. Yan, L. Quan, Y. Lan and Y. Gao, "Characteristics of delivery pressure in the axial piston pump with combination of variable displacement and variable speed", *Proc. Inst. Mech. Eng., Part I: J. Syst. Control Eng.*, Vol. 229, No. 7, pp. 599-613, (2015).

[15] N. D. Manring and R. C. Fales, *Hydraulic Control Systems*; 2nd ed, Wiley, New Jersey, pp. 1597-159, (2019).

[16] Q. Chao, Z. Xu, J. Tao and C. Liu, "Capped piston: A promising design to reduce compressibility effects, pressure ripple and cavitation for high-speed and high-pressure axial piston pumps", *Alex. Eng. J.*, Vol. 62, pp. 509-521, (2023). https://doi.org/10.1016/j.aej.2022.07.048

[17] F. Yin, S. Nie, W. Hou and S. Xiao, "Effect analysis of silencing grooves on pressure and vibration characteristics of seawater axial piston pump", *Proc. Inst. Mech. Eng., Part C: J. Mech. Eng. Sci.*, Vol. 231, No. 8, pp. 1390-1409, (2017).

[18] A. I. Nizhegorodov, A. N. Gavrilin, B. B. Moyzes, A. I. Cherkasov, O. M. Zharkevich, G. S. Zhetessova and N. A. Savelyeva, "Radial-piston pump for drive of test machines", *IOP Conf. Ser.: Mater. Sci. Eng.*, Vol. 289, No. 1, pp. 012014, (2018).

[19] P. Dong, S. Zhao, Y. Wang, P. Zhang, X. Han, C. Liu, D. Meng and Y. Dong, "Design and Experimental Study of Radial Piston Pump with Valve Plate Distribution", *Proc. ASME 2019, Int. Mech. Eng. Congress and Expo., Des., Syst., and Complx.*, Salt Lake City, Utah, USA, November 11–14, Vol. 14, V014T14A035, (2019).

[20] K. A. Harrison and K. A. Edge, "Reduction of axial piston pump pressure ripple", *Proc. Inst. Mech. Eng., Part I: J. Syst. Control Eng.*, Vol. 214, No. 1, pp. 53-64, (2000).

[21] S. G. Ye, J. H. Zhang and B. Xu, "Noise reduction of an axial piston pump by valve plate optimization", *Chin. J. Mech. Eng.*, V ol.31, No. 1, pp. 1-16, (2018).

[22] J. Zhou, C. Jing, Q. Bao and W. Wu, "Novel study on the pressure pulsation of the axial piston machines with even number of pistons", *The J. Eng.*, Vol. 2020, No. 14, pp. 932-935, (2020).

[23] J. Tao, H. Wang, H. Liao and S. Yu, "Mechanical design and numerical simulation of digital-displacement radial piston pump for multi-megawatt wind turbine drivetrain", *Renew. Energy*, Vol.143, pp. 995-1009, (2019).

[24] M. Zielinski, A. Myszkowski, M. Pelic and R. Staniek, "Low-speed radial piston pump as an effective alternative power transmission for small hydropower plants", *Renew. Energy*, Vol. 182, pp. 1012-1027, (2022).

[25] M. R. Aligoodarz, M., Dalvandi and A. Mehrpanahi, "Solid-phase effects on the performance of a centrifugal slurry pump using computational fluid dynamics", *J. Comput. Appl. Res. Mech. Eng. (JCARME)*, Vol. 11, No. 1, pp. 243-255, (2021).